Experimental Investigation On Hydrate Dissociation in Near-Wellbore Region Caused By Invasion of Drilling Fluid: Ultrasonic Measurement and Analysis

Qingchao Li (liqingchao2020@hpu.edu.cn)
Henan Polytechnic University https://orcid.org/0000-0001-7373-4046
Yuanfang Cheng
China University of Petroleum Huadong - Qingdao Campus
Ubedullah Ansari
Mehran University of Engineering & Technology
Ying Han
Henan Polytechnic University
Xiao Liu
Henan Polytechnic University
Chuanliang Yan
China University of Petroleum Huadong - Qingdao Campus

Research Article

Keywords: Hydrate-bearing sediments, Hydrate dissociation, Drilling fluid invasion, Methane leakage, marine environment, Ultrasonic measurement

Posted Date: November 19th, 2021

DOI: https://doi.org/10.21203/rs.3.rs-1018418/v1

Abstract

As we all know, development and utilization of clean energy is the only way for society to achieve sustainable development. Although natural gas hydrates is a new type of clean energy, uncontrollable hydrate dissociation and accompanying methane leakage in drilling operation threaten drilling safety and marine environment. However, dissociation range of natural gas hydrates around wellbore can't be reasonably and clearly determined in previous investigations, which may lead to the inaccurate estimation of borehole collapse and methane leakage. Then, the marine environment will be greatly damaged or affected. The purpose of the present work is to experimentally explore the dissociation characteristics of natural gas hydrates around wellbore in drilling operation, and analyze the influence law and mechanism of various factors on hydrate dissociation. It is expected to provide reference for exploring effective engineering measures to avoid the uncontrolled hydrate dissociation, borehole collapse and accompanying methane leakage. The experimental results demonstrate that acoustic velocity of hydrate-bearing sediment can be accurately expressed as quadratic polynomial of hydrate saturation, which is the theoretical basis for determination of hydrate saturation in subsequent experiments. Owing to the fact that hydrate dissociation is an endothermic reaction, hydrate dissociation gradually slows down in experiment. Throughout the experiment, the maximum dissociation rate at the beginning of the experiment is 8.69 times that at the end of the experiment. In addition, sensitivity analysis found that the increase of stabilizer concentration in drilling fluid can inhibit hydrate dissociation more than the increase in hydrate saturation. Hydrate dissociation was completely inhibited when the concentration of soybean lecithin exceeds 0.60wt%, but hydrate dissociation definitely occurs in the near-wellbore region no matter what hydrate saturation is. In this way, based on the requirements of drilling safety and environment protection, hydrate dissociation and accompanying methane leakage can be controlled by designing and adjusting the stabilizer concentration in drilling fluid.

Introduction

Natural gas hydrates are ice-like cage crystals composed of host water molecules and guest natural gas molecules (methane commonly consists more than 95%) under low temperature and high pressure conditions (Sloan 2003; Ye et al. 2018; Liu et al. 2021). In nature, gas hydrates are mainly buried in offshore sediments, and also diffused in a small amount in permafrost, the total global reserves amount to 2.1×10^{16} m^3 (Zhang et al. 2021; Gambelli 2021). In addition to huge reserves, utilization of natural gas hydrates is environmentally friendly, the combustion products are almost only carbon dioxide (CO_2) and water (H_2O) (Misyura 2020). Own to the above-mentioned two aspects, natural gas hydrates have been attracting significant global attention, a series of offshore trial production activities have been performed in recent years (Zhu et al. 2021; Sahu, Kumar and Sangwai, 2021). Among them, China's second production test in the South China Sea in 2020 achieved a satisfactory result of producing 8.614×10^5 m^3 of methane within one month (Ye et al. 2020; Zhu et al. 2021; Sahu, Kumar and Sangwai, 2021). It is believed that with the gradual improvement of exploitation techniques, natural gas hydrates are likely to

become a potential alternative energy source for oil and gas in the near future (Zhao et al. 2019b; Wang et al. 2021b).

Nevertheless, some issues will probably occur during drilling or exploitation of natural gas hydrates offshore (Yan et al. 2018; Song et al. 2019; Yan et al. 2020; Yang et al. 2021;Li et al. 2021a). Among them, as presented in Figure 1, hydrate dissociation around wellbore and borehole collapse caused by drilling fluid disturbance during drilling operation is one issue that can't be ignored (Li et al. 2020). As can be seen in Figure 1a, natural gas hydrates in the near-wellbore region are stable before or at the beginning of drilling operation, almost no hydrates dissociate (Li et al. 2021b). At this time, borehole stability can be well maintained because natural gas hydrates have not yet begun to dissociate and the sediment strength is high (Li et al. 2020a). However, the borehole directly or indirectly contacts with drilling fluid while drilling in hydrate reservoir, and invasion of drilling fluid into hydrate reservoir is inevitable (Salehabadi 2009). Generally speaking, disturbance of drilling fluid on reservoir temperature and reservoir pressure persists throughout the drilling operation (Golmohammadi and Nakhaee 2015). As demonstrated in Figure 1b, changes in sediment temperature and sediment pressure in the near-wellbore region will cause hydrate dissociation (Song et al. 2019), reduction of sediment strength (Yan et al. 2017; Cheng et al 2021; Yao et al. 2021), and borehole instability (Li et al. 2020). Borehole collapse will significantly affect the subsequent cementing operation, and the cementing quality will decline to a certain extent. In this case, the integrity of wellbore is extremely difficult to guarantee during methane production from natural gas hydrates (Salehabadi 2009). What's more, borehole collapse will also prolong the drilling cycle and increase the drilling costs (Ashena et al. 2020; Zhao et al. 2019a). The gas produced in offshore drilling operation is usually directly discharged into the atmosphere, so methane leakage caused by uncontrollable hydrate dissociation is also an important environmental issue during drilling operation in hydrate reservoir. Fortunately, adding appropriate concentrations of stabilizers (such as lecithin) to the drilling fluid can alleviate this situation to a certain extent (Zhao et al. 2019b; Wang et al. 2021a). Therefore, it is of great importance to perform experimental and theoretical studies on stability of gas hydrates around wellbore for safe and efficient drilling operation in hydrate reservoir, as well as protection of marine environment.

During recent years, several studies regarding the effect of drilling fluid on hydrate reservoir during drilling operation have been performed. All these studies are helpful to further explore the engineering measures to prevent excessive hydrate dissociation around wellbore and uncontrollable wellbore instability during drilling operation in hydrate-bearing sediments. To name a few, Huang et al. (2020) experimentally explored the disturbance of drilling fluid with different circulation rates on hydrate-bearing sediments in drilling operation, and found that both the temperature increase region around wellbore and gas production increase with the increase of circulation rate. Gao et al. (2019) measured the temperature change of hydrate-bearing sediments around wellbore in drilling operation, indicating that heat transfer in hydrate reservoir can be divided into six periods, which is complex than that in conventional reservoir. Yu et al. (2018) investigated gas production from hydrates and gas kick during drilling through hydrate reservoir, and the results show that hydrate dissociation was significantly affected by factors such as drilling fluid temperature and pressure. Freij-Ayoub et al. (2007) inspected both hydrate dissociation and

wellbore stability in hydrate reservoir by developing a coupling model, and found that physical field was an important factor affecting hydrate dissociation in hydrate deposits. Ning et al. (2013) numerically analyzed the effect of drilling fluid invasion on reservoir temperature, reservoir pressure and hydrate dissociation by using a 1D model. The simulation results show that the disturbance of drilling fluid invasion on hydrate stability is related not only to the drilling fluid properties, but also to reservoir characteristics.

To the best of the authors' knowledge, there are two shortcomings in previous investigations. For one thing, relevant experimental investigations mainly focus on the influence of drilling fluid disturbance on reservoir temperature and reservoir pressure in the near-wellbore region, rather than its impact on hydrate dissociation. Even if there are some studies on hydrate dissociation around wellbore in drilling operation, hydrate dissociation is indirectly described by gas production, rather than directly by distribution of hydrate saturation. In this way, dissociation range of gas hydrates around wellbore in previous experimental studies is difficult to be accurately determined. It should be noted that borehole collapse is difficult to be reasonably evaluated if dissociation range of gas hydrates around wellbore is not clear, because mechanical properties of hydrate deposits are directly related to hydrate saturation. For another, although some numerical investigations directly presented the distribution of hydrate saturation around wellbore in drilling operation, the simulation results are usually lack of credibility verification. In short, despite the fact that some progress has been made in current research, further exploration and improvement are still needed. Most importantly, the formation and dissociation of gas hydrates in sediments are difficult to be observed through human eyes. Therefore, it is necessary to experimentally illustrate hydrate dissociation around wellbore while drilling in hydrate reservoir directly through hydrate saturation by certain technical means.

Inspired by the previous studies, an apparatus was designed for directly investigating hydrate dissociation around wellbore in drilling operation by measuring distribution of hydrate saturation in sediment. First, relationship between hydrate saturation in sediment and P-wave velocity was determined with experiments, which could serve as the basis for determining hydrate saturation according to P-wave velocity obtained in experiments. Then, evolution characteristics of hydrate dissociation around wellbore caused by drilling fluid disturbance during drilling operation in hydrate-bearing sediments were explored in detail. Finally, in order to lay the foundation for putting forward practical engineering measures to avoid wellbore instability and uncontrollable methane leakage, factors (such as stabilizer concentration and hydrate saturation) affecting hydrate dissociation around wellbore were investigated. This work provides basic experimental data for numerical prediction of both borehole collapse and methane leakage in hydrate reservoir offshore, as well as verification of the relevant multi-fields coupled simulation model.

Experimental Section

2.1 Materials

Methane (CH4, 99.99% purity) supplied by Zhengzhou Xingdao Chemical Technology Co., Ltd. was used for hydrate preparation in this study. The low-viscosity polyanionic cellulose (PAC-LV), amphoteric polymer (FA-367) and sulfonated phenolic resin (SMP), as additives of water-based drilling fluid,[11] were all provided by Sinopec Offshore Oil Engineering Co., Ltd. The soybean lecithin was donated by Nanjing Ruize Fine Chemical Co., Ltd, and it was used as hydrate stabilizer. Marine soil used for preparation of hydrate-bearing sediment was obtained in Shenhu area of the South China Sea, and was provided by the Institute of Deep-sea Science and Engineering, CAS.

2.2 Experimental apparatus

Figure 2 illustrates the piping and instrumentation diagram of the experimental apparatus used in this study. Both in-situ preparation of hydrate-bearing sediments and hydrate dissociation experiments can be conducted with this apparatus. The apparatus mainly consists of a hydrate in-situ formation and dissociation unit, a fluid circulating unit, a pressure controlling unit and an ultrasonic measurement system. The autoclave (radius: 31cm, height: 6cm, wall thickness: 1cm, material: 316L stainless steel) filled with sediments needs to be placed in cold storage (refrigeration limit: -50℃) throughout the experiment, and its inlet is connected to a methane cylinder by needle valve 2. During preparation of hydrate-bearing sediments, sufficient methane can be continuously supplied to the sediment in autoclave by the methane cylinder (volume: 40L). A gas-liquid separator is connected with the outlet of autoclave, and the dissociation gas can be effectively separated and measured from the gas-liquid mixture in circulating pipeline. The circulating pump (maximum flow: 5.0L/min, weight: 5.2kg) connected with the separator can realize constant-flow circulation of drilling fluid in apparatus, and the flow rate in all experiments is 2.0L/min. The temperature control tank (volume: 20L) can heat and insulate the drilling fluid circulated in apparatus, and the heating limit is 100℃. The pressure control unit is composed of two servo pumps (precision: 0.05l/min), which can be used for controlling the bottom hole pressure and the reservoir pressure respectively.

The ultrasonic measurement system (frequency range: 0.01-1.00MHz) is the apparatus core, and it is purchased from Yangzhou Oriental Ultrasound Technology Co., Ltd. Figure 3 shows the schematic of measurement principle of ultrasonic measurement system. As highlighted in Figure 3a and b, 40 sets of transducers are evenly arranged on the upper and lower surfaces of the autoclave in five radial paths. The distance between two adjacent transducers in one radial path is 3.0cm. As shown in Figure 3c and d, in experiment, the ultrasonic is excited by the transmitting transducer, and received by the receiving transducer after being attenuated by sediment. Then, the received acoustic wave velocity was automatically transmitted back to the acoustic measurement system for data processing.

2.3 Experimental mthod

The whole experiment roughly covered two steps: preparation of hydrate-bearing sediment, and hydrate dissociation experiment. The research framework is presented in Figure 4, and the detailed description of experimental method was performed in this section.

2.3.1 Preparation of hydrate-bearing sediments

The reaction of methane and water to form methane hydrate at low temperature and/or high pressure can be expressed as (Joseph et al. 2017):

$CH_4 + nH_2O \leftrightarrow CH_4 \cdot nH_2O$ (Reaction 1)

Hydrate-bearing sediments were prepared in laboratory by using the marine soil obtained in the study area, and Figure 5 shows the preparation process. As displayed in Figure 5, the "excess gas method" was used to prepare hydrate-bearing sediments in this study (Sell et al. 2016). During the preparation, the marine soil needs to be dried and crushed (particle structure should not be destroyed) first. Then, distilled water with mass of m_w is measured and fully mixed with the dry soil in autoclave. The mass of water m_w was determined by Eqs. (1):

$$m_w = \frac{207}{239} V \varphi S_h \rho_h \quad (1)$$

where V is the internal volume of autoclave, φ is the porosity of hydrate-bearing sediment, S_h is hydrate saturation, and ρ_h is hydrate density (0.91g/cm^3).

After that, the mixture of water and soil in autoclave is compacted with a pressure of about 2.80MPa. The purpose is to restore the compaction state of sediments in shallow environment at a depth of ~200m below the seafloor. Finally, adjust the experimental temperature in cold storage below the phase equilibrium temperature, and continuously inject sufficient methane into autoclave until the autoclave pressure is constant. Preparation time of hydrate-bearing sediments may last for ~1 to 3 days, which depends on hydrate saturation. In this study, seven hydrate-bearing sediments with hydrate saturation of 0, 0.08, 0.16, 0.24, 0.32, 0.40 and 0.48 were prepared.

2.3.2 Experiment of hydrate dissociation

After all hydrate-bearing sediments were prepared, relationship between acoustic velocity and hydrate saturation should be obtained. Then, experiment of hydrate dissociation can be conducted by closing valve 2 and opening other valves.

During hydrate dissociation experiment, drilling fluid was heated first in temperature control tank for ~1h until its temperature reaches the required experimental temperature. Then, circulating pump was turned on, and its flow rate was stabilized as 2L/min. Two minutes later, temperature in cold storage and pore pressure of hydrate-bearing sediment in autoclave were adjusted to 15.25℃ (initial reservoir temperature) and 15.50MPa (initial reservoir pressure) respectively. Finally, the two-day experiment was started by adjusting the bottom-hole pressure to the experimental value through the mud pressure control pump. During the experiment, the wave velocities were recorded once every 10 minutes by the ultrasonic measurement system. The received acoustic velocity was converted to hydrate saturation by Eqs. (2) in ultrasonic measurement system.

$S_h = P_v(S_h)$ (2)

where $P_v(S_h)$ is the function describing relationship between P-wave velocity and hydrate saturation obtained in experiment.

Results And Discussion

3.1 Relationship between hydrate saturation and P-wave velocity

As mentioned above, hydrate dissociation around wellbore during drilling operation was assessed through distribution of hydrate saturation. Before hydrate dissociation experiment, relationship between hydrate saturation and acoustic velocity (i.e., $P_v(S_h)$ in Eqs. (2)) needs to be explored first. To highlight the representativeness of experimental data, 8 of 40 transducers were randomly turned on every time the acoustic velocity measurement was conducted for hydrate-bearing sediment with specific hydrate saturation. The measurement results of acoustic velocity are given in Table 1. As observed in Table 1, for sediment with specific hydrate saturation, 8 velocity data present little difference.

Table 1 Measurement results for hydrate-bearing sediment with specific hydrate saturation

Transducers No.	Acoustic velocity of hydrate-bearing sediments with different S_h, km/s						
	S_h=0	S_h=0.08	S_h=0.16	S_h=0.24	S_h=0.32	S_h=0.40	S_h=0.48
1	1.397	1.433	1.541	1.787	2.065	2.418	2.853
2	1.393	1.438	1.536	1.783	2.062	2.407	2.846
3	1.391	1.429	1.539	1.786	2.057	2.426	2.848
4	1.402	1.431	1.538	1.791	2.069	2.415	2.842
5	1.395	1.435	1.543	1.788	2.062	2.410	2.840
6	1.389	1.436	1.542	1.784	2.071	2.421	2.845
7	1.401	1.435	1.544	1.776	2.063	2.418	2.838
8	1.406	1.432	1.540	1.793	2.067	2.416	2.861

However, statistical significance test is the premise for obtaining function $P_v(S_h)$. To this end, the statistical analysis was conducted with “One way ANOVA” in IBM SPSS Statistics 25. The results of error analysis and significance analysis are shown in Table 2 and Table 3 respectively. From Table 2, we can see that the maximum standard error and maximum standard deviation are only 0.002645 and 0.007482 respectively. The errors may be caused by the slight lateral difference in hydrate saturation in sediment during preparation of hydrate-bearing sediment. Additionally, as observed in Table 3, the significance Ps

0.000, which is less than 0.050. Therefore, effect of hydrate saturation on acoustic velocity of sediment is statistically significant (F=96598.507, P=0.000<0.050).

Table 2 Error analysis results

Items	S_h=0	S_h=0.08	S_h=0.16	S_h=0.24	S_h=0.32	S_h=0.40	S_h=0.48
Average value, km/s	1.3968	1.4336	1.5404	1.7871	2.0645	2.4164	2.8466
Standard deviation	0.005874	0.002925	0.002669	0.003441	0.004472	0.005975	0.007482
Standard error	0.002077	0.001034	0.000944	0.001217	0.001581	0.002112	0.002645

Table 3 Significance test results (One way ANOVA)

	Sum of squares	df	Mean square	F	Significance, P
Between group	14.382	6	2.397	96598.508	0.000
In group	0.001	48	0.000	-	-

Taking the average acoustic velocity as the standard, Figure 6 displays the relationship between acoustic velocity and hydrate saturation. It can be found from Figure 6 that acoustic velocity increases with hydrate saturation in the form of a nonlinear quadratic function. However, the specific quantification needs to be achieved through data fitting. After fitting operation in Excel, relationship between acoustic velocity and hydrate saturation was expressed by Eqs. (3).

$$P_v(S_h) = 0.0006S_h^2 + 0.0015S_h + 1.3874 \qquad (R^2 = 0.9994) \tag{3}$$

Notably, for Eqs. (3), the correlation coefficient R^2 is 0.994, indicating that hydrate saturation can be determined by inversion of acoustic velocity obtained in hydrate dissociation experiments.

3.2 Evolution characteristics of hydrate dissociation around wellbore

Hydrate dissociation is an important factor causing wellbore instability while drilling in hydrate reservoir. Therefore, it's necessary to deeply explore the evolution characteristics of hydrate dissociation around wellbore during the drilling operation. Based on the experimental conditions (default case) in Table 4, Figure 7 displays the distribution nephogram of hydrate saturation in sediment at different experimental moments. As observed in Figure 7, hydrate saturation at the position with the same distance from borehole on any path is basically equal to each other at the same experimental moment. Therefore, distribution of hydrate saturation in sediment during the experiment can be represented by that on any

path. In this study, experiments are all based on the conditions shown in Table 4if no specific statement is made.

Table 4 Experimental conditions of default case

Experimental condition	Unit	Value
Hydrate saturation	-	0.24
Stabilizer concentration	wt%	0.30
Mud pressure	MPa	14.84
Mud temperature	K	296.40
Environment temperature	K	288.40
Reservoir pressure	MPa	14.55
Circulation flow rate	L/min	2.0
Total experimental time	h	48

Figure 8 demonstrates the distribution evolution of hydrate saturation along Path-1 around wellbore. From Figure 8, we can see that dissociation of natural gas hydrates firstly occurs in area near borehole due to the disturbance of drilling fluid at the beginning of experiment. When the experiment goes on for 0.5 hours, hydrate saturation at the borehole wall decreases to 0.172, and width of the dissociation transition area is 0.52 times the borehole radius (expressed as $0.52r_b$). After that, caused by the continuous disturbance of drilling fluid, hydrate dissociation gradually occurs outward along the radial direction, and the dissociation transition area thereby widens. When the experiment has lasted for 1.0h and 4.0h, width of the dissociation transition area reaches $1.13r_b$ and $2.96r_b$ respectively. However, natural gas hydrates at the borehole wall don't completely dissociate until 12.0 hours after the experiment starts, which means that the completely dissociation area appears since this moment. Meanwhile, width of the dissociation transition area is $5.91r_b$ when the experiment has lasted for 12.0 hours. In addition, with the continuation of the experiment, hydrate dissociation continues to occur at locations further away from the borehole. When the experiment was over, width of the completely dissociation area has reached $1.34r_b$, and the rest of the sediment is in the dissociation transition area.

During the experiment, the dissociation rate of natural gas hydrates is not constant. The dissociation rate of natural gas hydrate along Path-1 for different experimental moments is as shown in Figure 9. Notably, the dissociation rate of natural gas hydrates used herein is obtained by:

$$D_v = \frac{dS_h}{dt} \quad (4)$$

where, dt is time interval, dS_h is the change of hydrate saturation in dt time interval.
As observed in Figure 9, at the beginning of the experiment, gas hydrates in area near borehole dissociate fastest. The maximum dissociation rate is $0.0113s^{-1}$ when the experiment goes on for 0.5 hours, and the position where gas hydrates dissociate fastest is the borehole wall. As the experiment remains, the position where fastest hydrate dissociation occurs gradually moves away from the borehole, and the maximum dissociation rate also dropped sharply. At the experimental moment of 12.0 hours, the maximum dissociation rate is $0.0032s^{-1}$, which is only 28.32% of that when the experiment is carried out for 0.5 hours. What's more, at the end of the experiment, positions with the maximum hydrate dissociation rate are about $4.25r_b$ away from the borehole wall, and the maximum hydrate dissociation rate has been only 0.0013 s^{-1}. Thereby, it can be inferred from Figure 9 that if the experiment continues after two days, hydrate dissociation rate at all positions will be lower. The mechanism why hydrate dissociation gradually weakens in experiment can be explained by Figure 10. As observed in Figure 10, hydrate dissociation is an endothermic reaction, so hydrate dissociation will cause the decrease in reservoir temperature. Besides, dissociation products (mainly methane and water) of gas hydrates can also lead to the increase in local pore pressure. Both the decrease in reservoir temperature and the increase in pore pressure caused by hydrate dissociation will inhibit its further dissociation. Furthermore, the above changes of reservoir temperature and pore pressure caused by hydrate dissociation will also restrain the heat transfer to the position farther away from the borehole. Thereby, hydrate dissociation at the position farther away from borehole will also be suppressed at the subsequent experimental moments.

3.3 Comparison of the present experimental study with published simulation works

As mentioned in introduction, this study can provide basic experimental data for verification of some numerical simulation models that used for the investigation of hydrate dissociation around wellbore. Therefore, differences between results of the present experimental investigation and the previous simulations should be explored in detail. Comparison of the experimental results with those obtained by two numerical simulation models in published works has been conducted in this section, and the comparison results are demonstrated as Figure 11.

As what we can see in Figure 11, there are some differences between results of two numerical simulations and this experimental investigation. Among them, the most significant difference is the width of the dissociation transition area. In both numerical simulations in Figure 11, width of the dissociation transition area is significantly compressed and is relatively constant throughout the simulation. For the simulation based on the model given by Freij-Ayob et al. (2007), width of the dissociation transition area is almost always maintained at about $1.15r_b$ during the whole simulation. Similarly, for the simulation based on the model given by Ning et al. (2013), in the whole simulation, width of the dissociation transition area is maintained at about $1.31r_b$. However, width of the dissociation transition area at any experimental moments is obviously wider than that in both numerical simulation. Moreover, width of the

dissociation transition area becomes wider and wider as the experiment continues. At 4.0h, 12.0h and 24.0h, width of the dissociation transition area in the present experiment is $3.36r_b$, $5.71r_b$ and $8.68r_b$. At 48.0h, the position where gas hydrates begin to dissociate is no longer in sediment, so width of the dissociation transition area at this experimental moment is not discussed. Yet, it can be inferred from Figure 11d that the width of the dissociation transition area is undoubtedly greater than $8.68r_b$ at the end of the experiment.

From Figure 11, we can also find that the positions where gas hydrates start to dissociate are almost the same in two numerical simulations, as well as in the experiment. However, we have already known that width of the dissociation transition area is obviously different from each other between the present experiment and previous numerical simulations. Thereby, range of the completely dissociation area obtained by experiment is naturally different from that obtained by previous simulations. As previously mentioned, in experiment, gas hydrates at borehole wall don't completely dissociate until 12.0 hours after the experiment starts, and the final range of the completely dissociation area is only $1.34r_b$. However, for both numerical simulations in Figure 11, gas hydrates at the borehole wall have completely dissociated at the beginning of simulation. Moreover, as two simulations continue, range of the completely dissociation area will gradually expand. For simulation based on a model developed by Freij-Ayob et al. (2007), range of the completely dissociation area is $2.75r_b$, $4.15r_b$, $6.32r_b$, and $8.25r_b$ respectively at 4.0h, 12.0h, 24h, and 48h. Likewise, for simulation based on a model developed by Ning et al. (2013), range of the completely dissociation area is $2.14r_b$, $3.56r_b$, $5.63r_b$, and $7.65r_b$ respectively at 4.0h, 12.0h, 24h, and 48h.

Actually, the difference between the experimental results and the simulation results is mainly attributed to the inappropriate understanding of the dissociation mode in numerical modeling. In numerical simulations, it is generally assumed that hydrate dissociation gradually advances outward from the borehole wall in the form of "thin piston", and the "thin piston" is exactly the dissociation transition area. Besides, It is also believed that natural gas hydrate in dissociation transition area can rapidly dissociate in numerical modeling, so that the dissociation transition area can move outward to the next position. Therefore, as observed in Figure 11, width of the dissociation transition area is basically unchanged throughout the simulation, and the completely dissociation area can appear rapidly and widen continuously. In fact, this is not exactly the case. In drilling operation, natural gas hydrates in the near-wellbore region dissociate outward in the form of a gradually widening dissociation transition area, not the form of "thin piston". Inaccurate simulation of hydrate dissociation affects the accuracy of borehole stability prediction. Thereby, in numerical modeling of hydrate dissociation around wellbore, not only more conditions need to be considered, but also the dissociation mode needs to be further modified.

3.4 Hydrate dissociation for sediments with different hydrate saturation

Borehole stability can be influenced by hydrate saturation through affecting hydrate dissociation around wellbore. Therefore, investigations on hydrate dissociation in hydrate-bearing sediments with different hydrate saturations need to be conducted.

In this section, effect of hydrate saturation on hydrate dissociation in the near-wellbore region was investigated, and the experimental result was displayed in Figure 12. As observed in Figure 12, for all hydrate saturations studied herein, hydrates at any position of the sediment have begun to dissociate or have completely dissociated at the end of experiment. It can also be seen from Figure 12 that dissociation of natural gas hydrates in sediments weakens nonlinearly with the increase of hydrate saturation. In range of low hydrate saturation ($S_h \leq 0.24$), hydrate dissociation weakens so obviously with the increase of hydrate saturation. If range of the completely dissociation area is used to describe it, final range of the completely dissociation area narrows rapidly within range of low hydrate saturation as the hydrate saturation increases. When hydrate saturation is only 0.08, gas hydrates in sediments dissociate rapidly in experiment, and final range of the completely dissociation area reaches $4.28r_b$. However, when hydrate saturation has increases to 0.24, final range of the completely dissociation area has decreased to $1.34r_b$, which is $2.94r_b$ narrower than that when the hydrate saturation is 0.08. Notably, when hydrate saturation exceeds 0.24, the phenomenon that hydrate dissociation weakens as hydrate saturation increases has become less obvious. When hydrate saturation increases from 0.24 to 0.48, final range of the completely dissociation area only decreases from $1.34r_b$ to $0.53r_b$, and the decline is only $0.81r_b$. We can boldly infer that if hydrate saturation continues to increase, final width of the completely dissociation area will be narrower than $0.53r_b$.

Figure 13 schematically illustrates the reason why hydrate dissociation weakens with the increase of hydrate saturation in drilling operation. We all know that the heat required for completely dissociating the specific amount of gas hydrates is constant. As observed in Figure 13, for all cases, heat Q is assumed to be transferred into the cube infinitesimal element with side length dr in the same time interval dt. If hydrate saturation is high (see Figure 13a, assuming S_{hhigh}), the heat Q provided by drilling fluid can only make gas hydrates in sediment with width of dr' in infinitesimal element completely dissociate. However, if hydrate saturation is low (see Figure 13b, assuming S_{hlow}), the heat Q can make gas hydrates in sediment with width of dr'' in infinitesimal element completely dissociate. Relationship between dr'' and dr' can be expressed by Eqs. (5):

$$dr'' = dr' \frac{S_{hhigh}}{S_{hlow}} \quad (5)$$

Since S_{hhigh} is assumed to be higher than S_{hlow}, dr'' is always wider than dr'. And, the greater the difference between S_{hhigh} and S_{hlow}, the wider dr'' is than dr'.

3.5 Effect of stabilizer concentration on hydrate dissociation

As an environmentally friendly additive for drilling fluid, soybean lecithin is a by-product in the process of refining soybean oil and will not have a serious impact on the marine environment. So, soybean lecithin is a hydrate stabilizer worthy of recommendation. In the present study, effect of soybean lecithin

concentration on hydrate dissociation has also been investigated. Figure 14 displays the final width of the completely dissociation area and dissociation transition area when the stabilizer concentration in the drilling fluid is different. As we can see from Figure 14, width of the completely dissociation area decreases as the stabilizer concentration increases until it reaches 0. Width of the completely dissociation area is $6.42r_b$ when there is no soybean lecithin in drilling fluid. However, when the stabilizer concentration reaches 0.60wt%, not only width of the completely dissociation area, but also width of the dissociation transition area are both 0. In other words, when the concentration of soybean lecithin is higher than 0.60wt%, dissociation of natural gas hydrates in the near-wellbore region around wellbore can be completely prevented during drilling operation. All these indicate that, addition of soybean lecithin in drilling fluid will have a better inhibitory effect on dissociation of gas hydrates around wellbore in drilling operation.

Previous studies have shown that soybean lecithin does not affect the stability of hydrate by changing the thermodynamic equilibrium conditions (Chen et al. 2007). In fact, just as displayed in Figure 15, soybean lecithin inhibits hydrate dissociation by forming the mesh membrane on hydrate surface to limit mass transfer. Transfer of water and methane molecules from the hydrate surface to the fluid in pores is free if there is no soybean lecithin in drilling fluid (see Figure 15a). That is to say, the mass transfer resistance can almost be ignored when the concentration of soybean lecithin is 0. With the increase in concentration of soybean lecithin, the mass transfer resistance gradually increases due to the formation of mesh membrane on the hydrate surface. When its concentration is not very high, adjacent soybean lecithin molecules form local mesh membrane on hydrate surface (see Figure 15b). In this case, some of the water and methane molecules produced by hydrate dissociation are blocked on the hydrate surface by the mesh membrane, further dissociation of gas hydrates is inhibited to some extent. However, if the concentration of soybean lecithin is high enough, the mesh membrane formed by soybean lecithin can completely cover the hydrate surface (see Figure 15c). Transfer of almost all water and methane molecules from the hydrate surface to the fluid in pores is blocked, then no hydrate dissociation can continue to occur in the subsequent experiment.

3.6 Prevention of uncontrollable hydrate dissociation and accompanying methane leakage

As mentioned above, methane leakage caused by hydrate dissociation in drilling operation poses the threat to the marine environment and the marine organisms, as well as the drilling safety. To prevent the marine environmental issues such as borehole collapse or methane leakage while drilling in hydrate reservoir, reducing hydrate dissociation around wellbore is the key. Adding environmental friendly hydrate stabilizer (such as soybean lecithin) to drilling fluid is an environmental and effective measure. Nevertheless, the stabilizer concentration in drilling fluid needs to be designed in advance according to acceptable hydrate dissociation or methane leakage. In terms of the experimental conditions herein, if it is required that hydrate dissociation and methane leakage cannot occur in drilling operation, concentration of soybean lecithin needs to be higher than 0.60wt%. However, it is unrealistic not to allow hydrate dissociation and methane leakage during drilling operation. According to Figure 14, If hydrates in

sediment with a width of $0.5r_b$ around wellbore is allowed to completely dissociate, the concentration of soybean lecithin needs to be at least 0.39wt%. Similarly, through Figure 14, we can determine the lower limit of soybean lecithin concentration corresponding to any acceptable width of completely dissociation area required by marine environmental protection.

Conclusion

In this study, an experimental apparatus used for determination of hydrate saturation by ultrasonic measurement was designed and assembled, and the influence of various factors on hydrate dissociation around wellbore during drilling in hydrate reservoir was also investigated. In order to reduce drilling risk and marine environmental pollution, engineering recommendations to prevent uncontrollable hydrate dissociation and methane leakage are given according to the experimental results. Method for determination of hydrate saturation in hydrate-bearing sediment was obtained by fitting the relationship between hydrate saturation and acoustic velocity. Through error analysis, it is concluded that this method has high accuracy and can be used extensively to determine hydrate saturation in hydrate-bearing sediments. Comparison between the experimental results of hydrate dissociation with the simulation results obtained by the numerical model given in previous numerical studies reveals obvious difference between them. This concludes that the previous numerical model needs to be properly modified in terms of dissociation mode with reference to the experimental results when it was used in the future. In addition, although the increase of hydrate saturation and soybean lecithin concentration can both weaken hydrate dissociation in experiment, the latter has a better effect. Depending on Figure 14, if no hydrate dissociation was acceptable in both of drilling safety and environmental protection, concentration of soybean lecithin in drilling fluid should be at least 0.60wt%. Overall, no matter what the requirement for hydrate dissociation is, concentration of soybean lecithin in drilling fluid can be adjusted in real time according to Figure 14. Investigation in the present work not only helps to reduce the risk of drilling operation, but also provides technical support for reducing greenhouse gas emissions and protecting the marine environment.

Declarations

Ethical Approval

Not applicable

Consent to Participate

Not applicable

Consent to Publish

Not applicable

Authors Contributions

Li Qingchao, Ansari Ubedullah: Testing, data analysis. Li Qingchao, Han Ying, Liu Xiao: writing -original draft preparation. Yan Chuanliang, Cheng Yuanfang: reviewing and editing. Ansari Ubedullah: English grammar modification.

Funding

Not applicable

Competing Interests

Not applicable

Availability of data and materials

Not applicable

Acknowledgments

This work is financially supported by the Postdoctoral Program of Henan Polytechnic University (712108/210). Moreover, the conception and launch of this work are also supported by the Rock Mechanics Laboratory (RML) of China University of Petroleum (East China).

References

1. Ashena R, Elmgerbi A, Rasouli V, Ghalambor A, Rabiei M, Bahrami A (2020) Severe wellbore instability in a complex lithology formation necessitating casing while drilling and continuous circulation system. *J Pet Explor Prod Te* 10(4): 1511-1532. https://doi.org/10.1007/s13202-020-00834-3
2. Chen W, Patil S L, Kamath V A, Chukwu G A (2007) Effect of lecithin on methane hydrate formation. *Huagong Xuebao (Chin. Ed.)* 58(11): 2895-2900.
3. Cheng W, Lu C, Ning F, Jia M (2021) A coupled thermal-hydraulic-mechanical model for the kinetic dissociation of methane hydrate in a depressurizing well. *J Pet Sci Eng* 207: 109021. https://doi.org/10.1016/j.petrol.2021.109021
4. Freij-Ayoub R, Tan C, Clennell B, Tohidi B, Yang J. (2007) A wellbore stability model for hydrate bearing sediments. *J Pet Sci Eng* 57(1-2): 209-220. https://doi.org/10.1016/j.petrol.2005.10.011
5. Gambelli A M (2021) Analyses on CH_4 and CO_2 hydrate formation to define the optimal pressure for CO_2 injection to maximize the replacement efficiency into natural gas hydrate in presence of a silica-based natural porous medium, via depressurization techniques. *Chem Eng Process* 167: 108512. https://doi.org/10.1016/j.cep.2021.108512
6. Gao Y, Chen Y, Wang Z, Chen L, Zhao X, Sun B (2019) Experimental study on heat transfer in hydrate-bearing reservoirs during drilling processes. *Ocean Eng* 183: 262-269.

https://doi.org/10.1016/j.oceaneng.2019.04.092

7. Golmohammadi S, Nakhaee A (2015) A cylindrical model for hydrate dissociation near wellbore during drilling operations. *J Nat Gas Sci Eng* 27(part 3): 1641-1648. https://doi.org/10.1016/j.jngse.2015.10.032
8. Huang T, Li X, Zhang Y, Wang Y, Chen Z (2020) Experimental study of the drilling process in hydrate-bearing sediments under different circulation rates of drilling fluid. *J Pet Sci Eng* 189: 107001. https://doi.org/10.1016/j.petrol.2020.107001
9. Joseph J, Dangayach S, Singh D, Kumar P, Dewri S, Tandi C, Singh J (2017) Investigation on excess gas method for synthesis of methane gas hydrates. *J Nat Gas Sci Eng* 42: 203-215. https://doi.org/10.1016/j.jngse.2017.02.043
10. Li Q, Liu L, Yu B, Guo L, Shi S, Miao L (2021a) Borehole enlargement rate as a measure of borehole instability in hydrate reservoir and its relationship with drilling mud density. *J Pet Explor Prod Te* 11(3): 1185-1198. https://doi.org/10.1007/s13202-021-01097-2
11. Li Y, Liu C, Liao H, Lin D, Bu Q, Liu Z (2021b) Mechanical properties of the clayey-silty sediment-natural gas hydrate mixed system. *Nat Gas Ind B* 8(2): 154-162. https://doi.org/10.1016/j.ngib.2020.08.002
12. Liu W, Liu R, Zhang M, Liu Z, Lang C, Li Y (2021) Rheological properties of hydrate slurry formed from mudflows in south China Sea. *Energy Fuels* 35(13): 10575-10583. https://doi.org/10.1021/acs.energyfuels.1c01294
13. Li Y, Cheng Y, Yan C, Song L, Ren X (2020) Mechanical study on the wellbore stability of horizontal wells in natural gas hydrate reservoirs. *J Nat Gas Sci Eng* 79: 103359. https://doi.org/10.1016/j.jngse.2020.103359
14. Misyura S Y (2020) Developing the environmentally friendly technologies of combustion of gas hydrates. Reducing harmful emissions during combustion. *Environ Pollut* 265(Part A): 114871. https://doi.org/10.1016/j.envpol.2020.114871
15. Ning F, Zhang K, Wu N, Zhang L, Li G, Jiang G, Yu Y, Liu L, Qin Y (2013a) Invasion of drilling mud into gas-hydrate-bearing sediments. Part I: effect of drilling mud properties. *Geophys J Int* 193(3): 1370-1384. https://doi.org/10.1093/gji/ggt015
16. Ning F, Wu N, Yu Y, Zhang K, Jiang G, Zhang L, Sun J, Zheng M (2013b) Invasion of drilling mud into gas-hydrate-bearing sediments. Part II: Effects of geophysical properties of sediments. *Geophys J Int* 193(3), 1385-1398. https://doi.org/10.1093/gji/ggt016
17. Sahu C, Kumar R, Sangwai J (2021) A comprehensive review on well completion operations and artificial lift techniques for methane gas production from natural gas hydrate reservoirs. *Energy Fuels* 35(15): 11740-11760. https://doi.org/10.1021/acs.energyfuels.1c01437
18. Salehabadi M (2009) Hydrates in sediments: their role in wellbore/casing integrity and CO2 sequestration. Ph.D. Thesis; Heriot-Watt University.
19. Sell K, Saenger E, Falenty A, Chaouachi M, Haberthür D, Enzmann F, Kuhs W, Kersten M. (2016) On the path to the digital rock physics of gas hydrate-bearing sediments – processing of in situ

synchrotron-tomography data. *Solid Earth* 7: 1243-1258. https://doi.org/10.5194/se-7-1243-2016.

20. Sloan E D (2003) Fundamental principles and applications of natural gas hydrates. *Nature* 426(6964): 353-359. https://doi.org/10.1038/nature02135
21. Song B, Cheng Y, Yan C, Lyu Y, Wei J, Ding J, Li Y (2019) Seafloor subsidence response and submarine slope stability evaluation in response to hydrate dissociation. J. Nat. Gas Sci. Eng. 2019, 65: 197-211. https://doi.org/10.1016/j.jngse.2019.02.009
22. Wang L, Jiang G, Zhang X (2021a) Modeling and Molecular Simulation of Natural Gas Hydrate Stabilizers. *Eur J Remote Sens* 54(sup2): 21-32. https://doi.org/10.1080/22797254.2020.1738901
23. Wang Y, Lang X, Fan S, Wang S, Yu C, Li G (2021b) Review on enhanced technology of natural gas hydrate recovery by carbon dioxide replacement. *Energy Fuels* 35(5): 3659-3674. https://doi.org/10.1021/acs.energyfuels.0c04138
24. Yan C, Cheng Y, Li M, Han Z, Zhang H, Li Q, Teng F, Ding J (2017) Mechanical experiments and constitutive model of natural gas hydrate reservoirs. *Int J Hydrogen Energy* 42(31): 19810-19818. https://doi.org/10.1016/j.ijhydene.2017.06.135
25. Yan C, Yang L, Cheng Y, Wang W, Song B, Deng F, Feng Y (2018) Sand production evaluation during gas production from natural gas hydrates. *J Nat Gas Sci Eng* 57: 77-88. https://doi.org/10.1016/j.jngse.2018.07.006
26. Yan C, Ren X, Cheng Y, Song B, Li Y, Tian W (2020) Geomechanical issues in the exploitation of natural gas hydrate. *Gondwana Res* 81: 403-422. https://doi.org/10.1016/j.gr.2019.11.014
27. Yang L, Wang J, Yang Y, Sun G (2021) Numerical analysis of soil deformation and collapse due to hydrate decomposition. *ACS Omega* 6: 5335-5347. https://doi.org/10.1021/acsomega.0c05463
28. Yao Y, Wei M, Kang W. (2021) A review of wettability alteration using surfactants in carbonate reservoirs. *Adv Colloid Interfac*, 294: 102477. https://doi.org/10.1016/j.cis.2021.102477
29. Ye J, Qin X, Qiu H, Xie W, Lu H, Lu C, Zhou J, Liu J, Yang T, Cao J, Sa R (2018) Data report: molecular and isotopic compositions of the extracted gas from China's first offshore natural gas hydrate production test in south China Sea. *Energies* 11(10): 2793. https://doi.org/10.3390/en11102793
30. Ye J, Qin X, Xie W, Lu H, Ma B, Qiu H, Liang J, Lu J, Kuang Z, Lu C, Liang Q, Wei S, Yu Y, Liu C, Li B, Shen K, Shi H, Lu Q, Li J, Kou B, Song G, Li B, Zhang H, Lu H, Ma C, Dong Y, Bian H (2020) The second natural gas hydrate production test in the south China Sea. *China Geology* 3(2): 197-209. https://doi.org/10.31035/cg2020043
31. Yu L, Xu Y, Gong Z, Huang F, Zhang L, Ren S (2018) Experimental study and numerical modeling of methane hydrate dissociation and gas invasion during drilling through hydrate bearing formations. *J Pet Sci Eng* 168: 507-520. https://doi.org/10.1016/j.petrol.2018.05.046
32. Zhang J, Sun Q, Wang Z, Wang J, Sun X, Liu Z, Sun B, Sun J (2021) Prediction of hydrate formation and plugging in the trial production pipes of offshore natural gas hydrates. *J Clean Prod* 316 (20): 128262. https://doi.org/10.1016/j.jclepro.2021.128262
33. Zhao X, Qiu Z, Wang M, Xu J, Huang W (2019a) Experimental investigation of the effect of drilling fluid on wellbore stability in shallow unconsolidated formations in deep water. *J Pet Sci Eng* 175:

595-603. https://doi.org/10.1016/j.petrol.2018.12.067

34. Zhao X, Qiu Z, Zhao C, Xu J, Zhang Y (2019b) Inhibitory effect of water-based drilling fluid on methane hydrate dissociation. *Chem Eng Sci* 199: 113-122. https://doi.org/10.1016/j.ces.2018.12.057
35. Zhu Y, Wang P, Pang S, Zhang S, Xiao R (2021) A review of the resource and test production of natural gas hydrates in China. *Energy Fuels* 35(11): 9137-9150. https://doi.org/10.1021/acs.energyfuels.1c00485

Figures

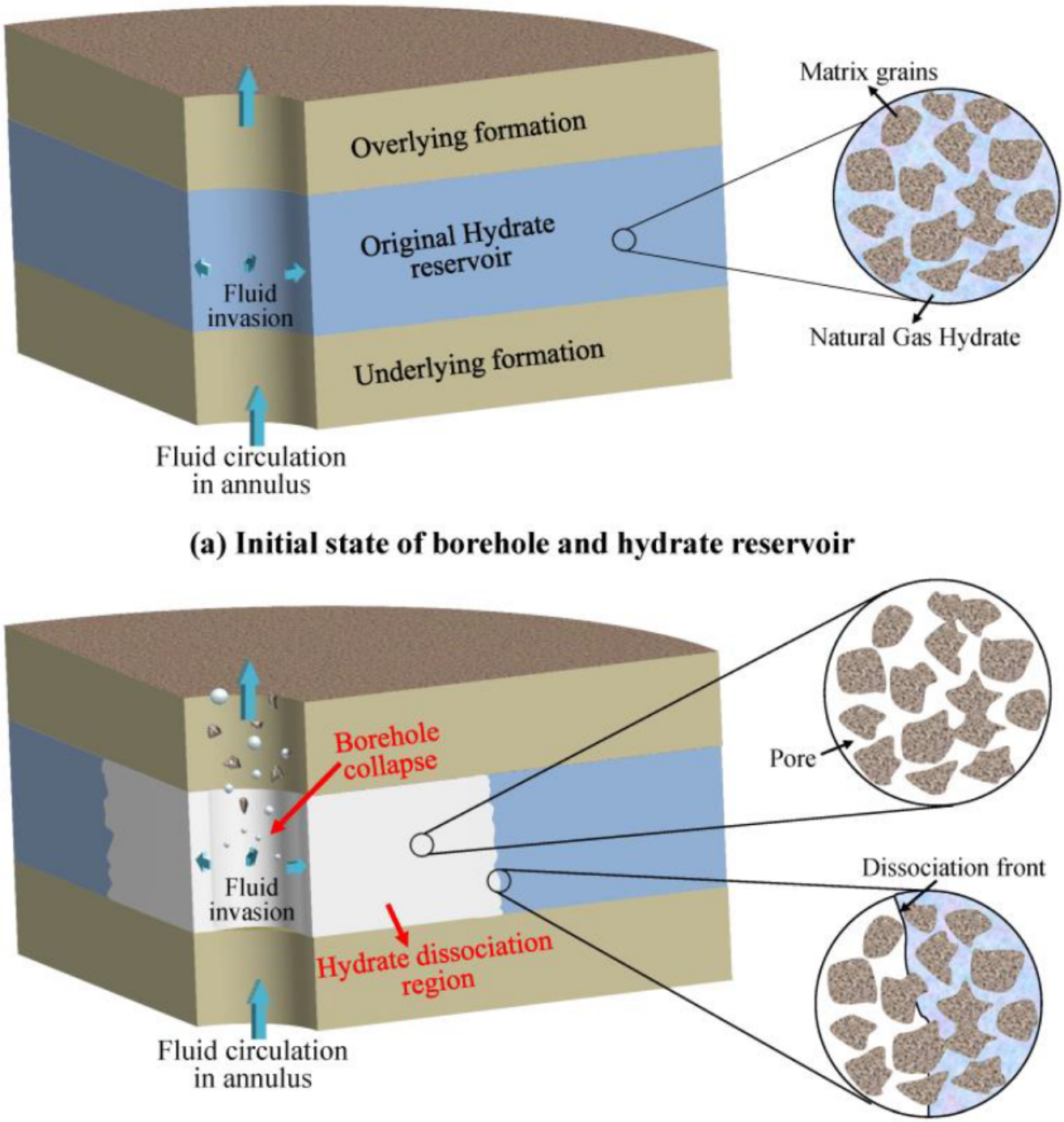

Figure 1

Hydrate dissociation around wellbore and borehole collapse while drilling in hydrate reservoir

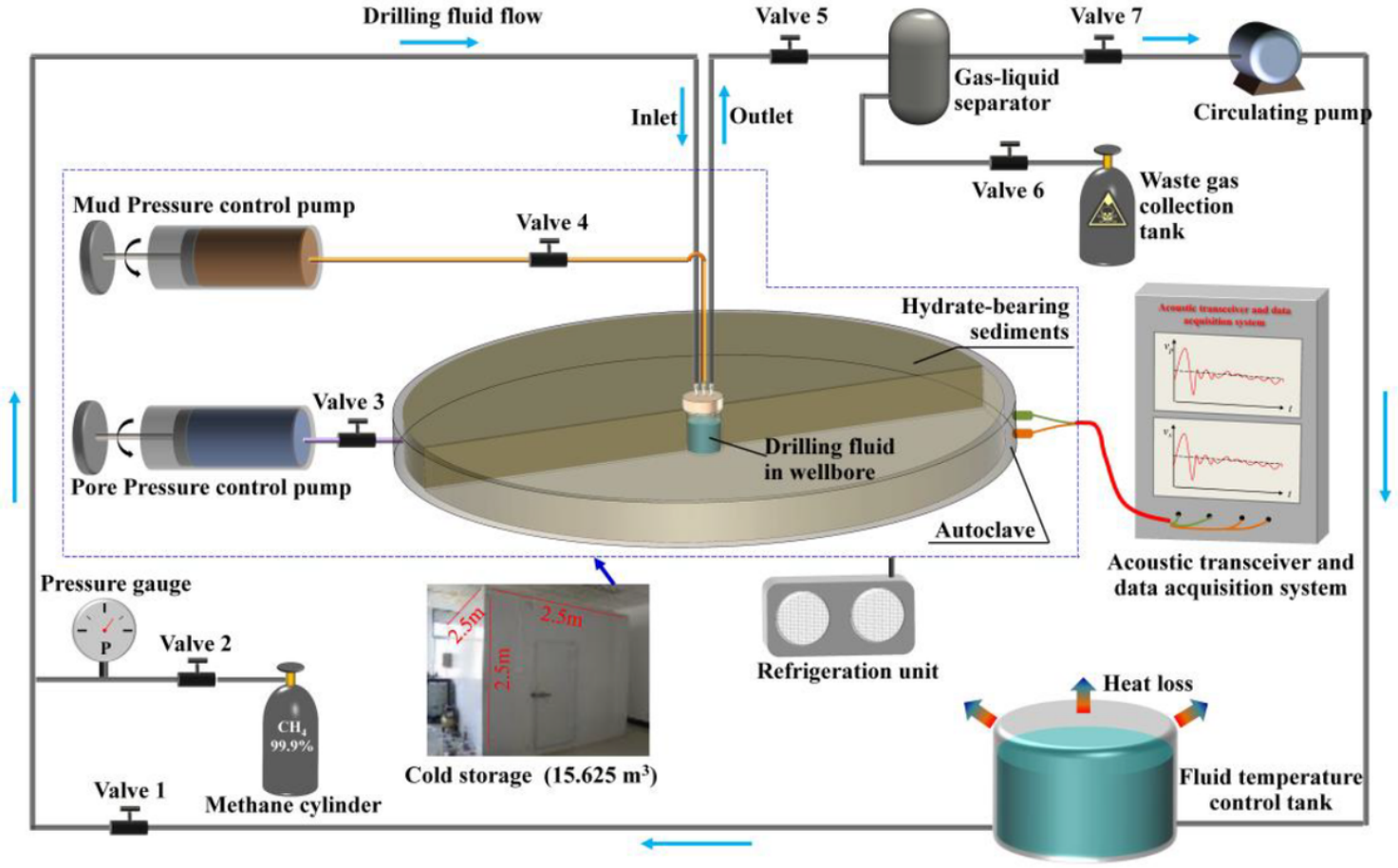

Figure 2

Piping and instrumentation diagram of the experimental system used in this paper

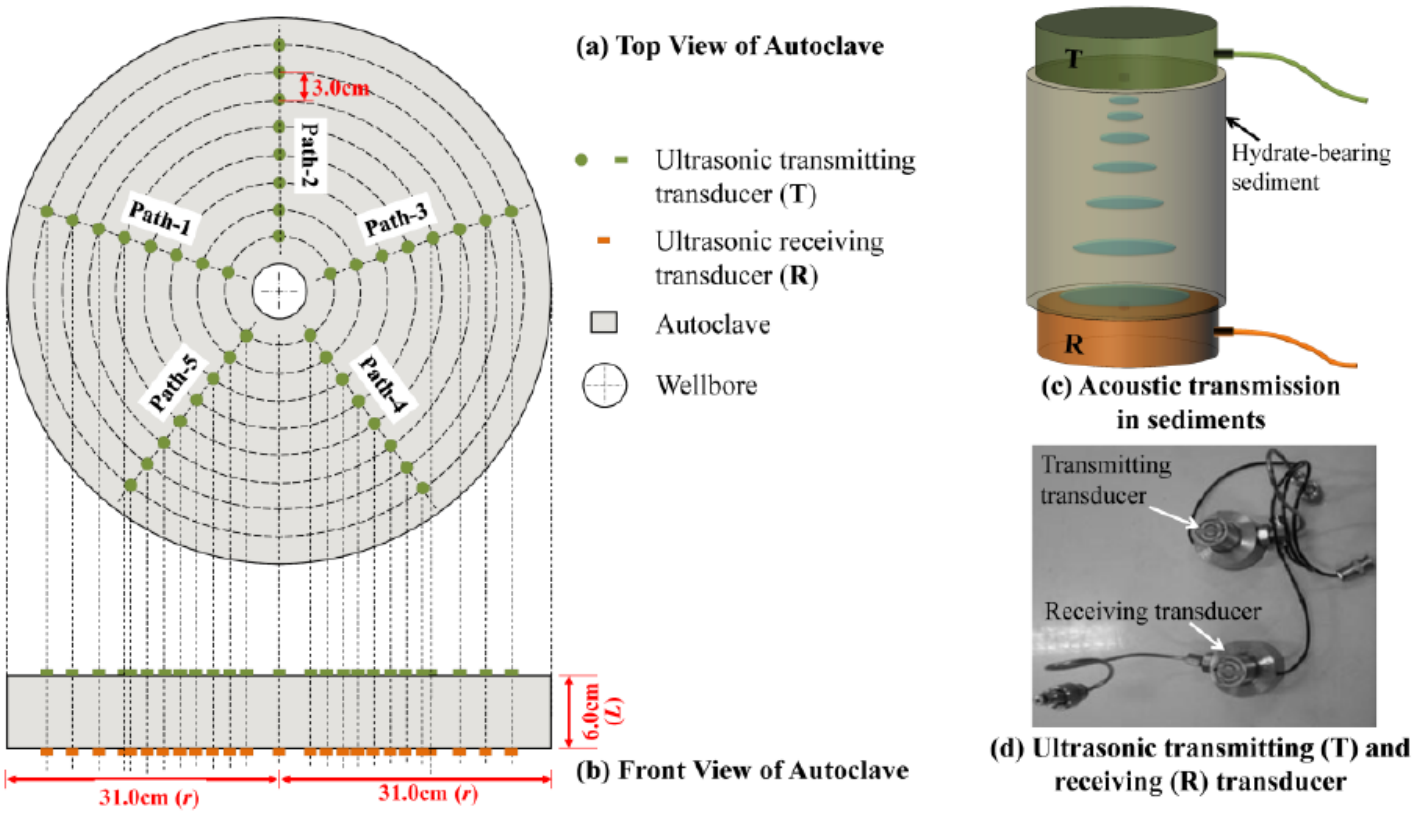

Figure 3

Installation and measurement principle of ultrasonic receiving transducer (R) and transmitting transducer (T)

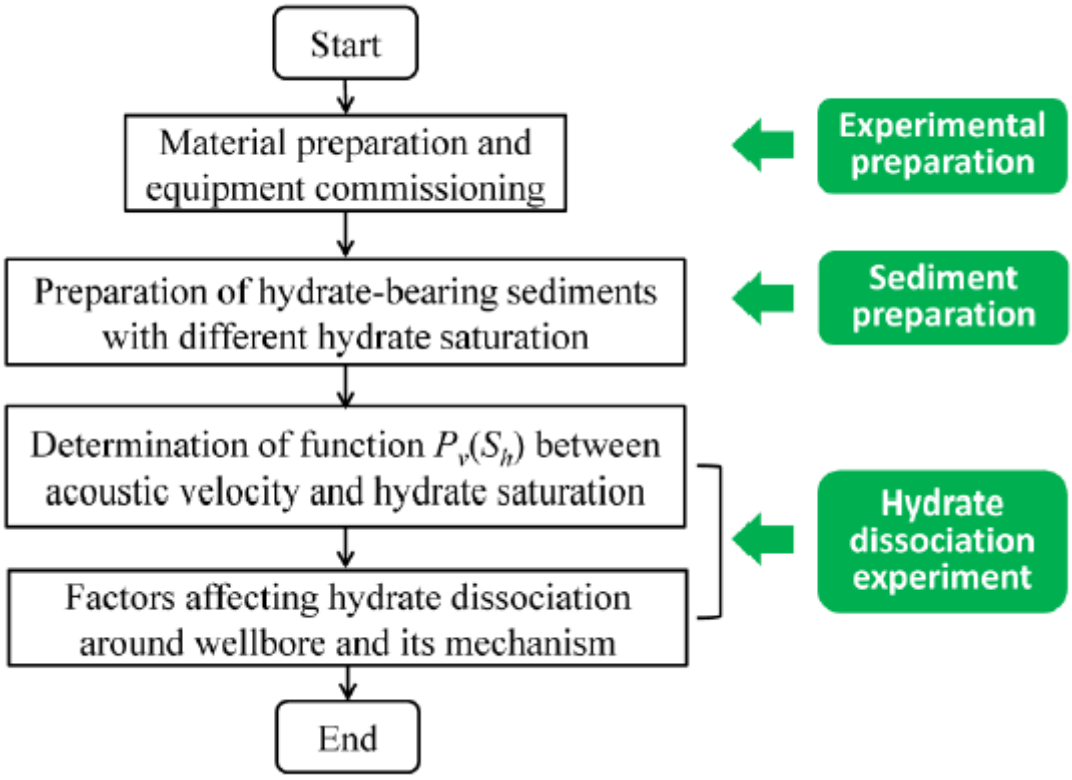

Figure 4

The research framework in the present work

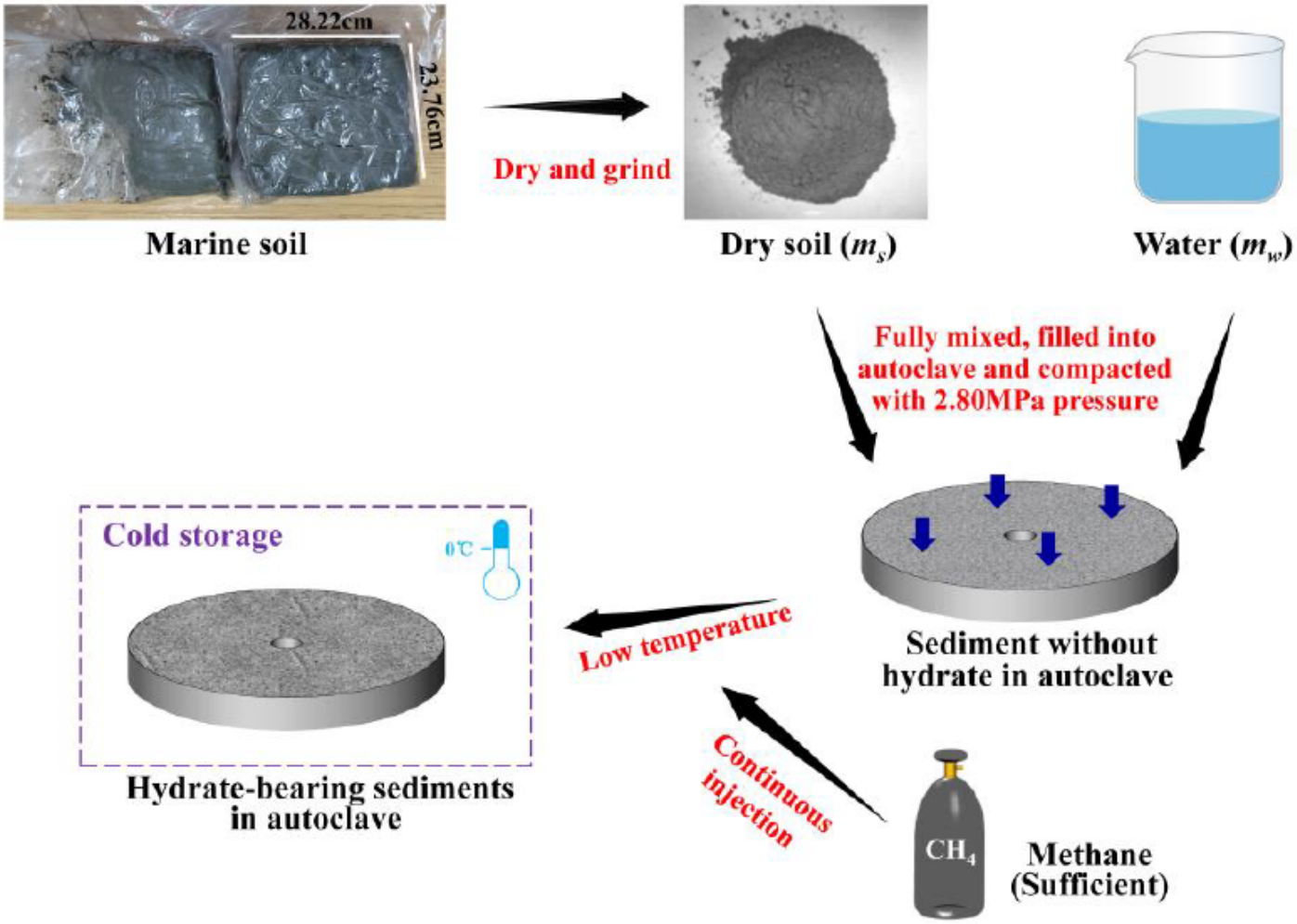

Figure 5

Preparation procedure of hydrate-bearing sediments

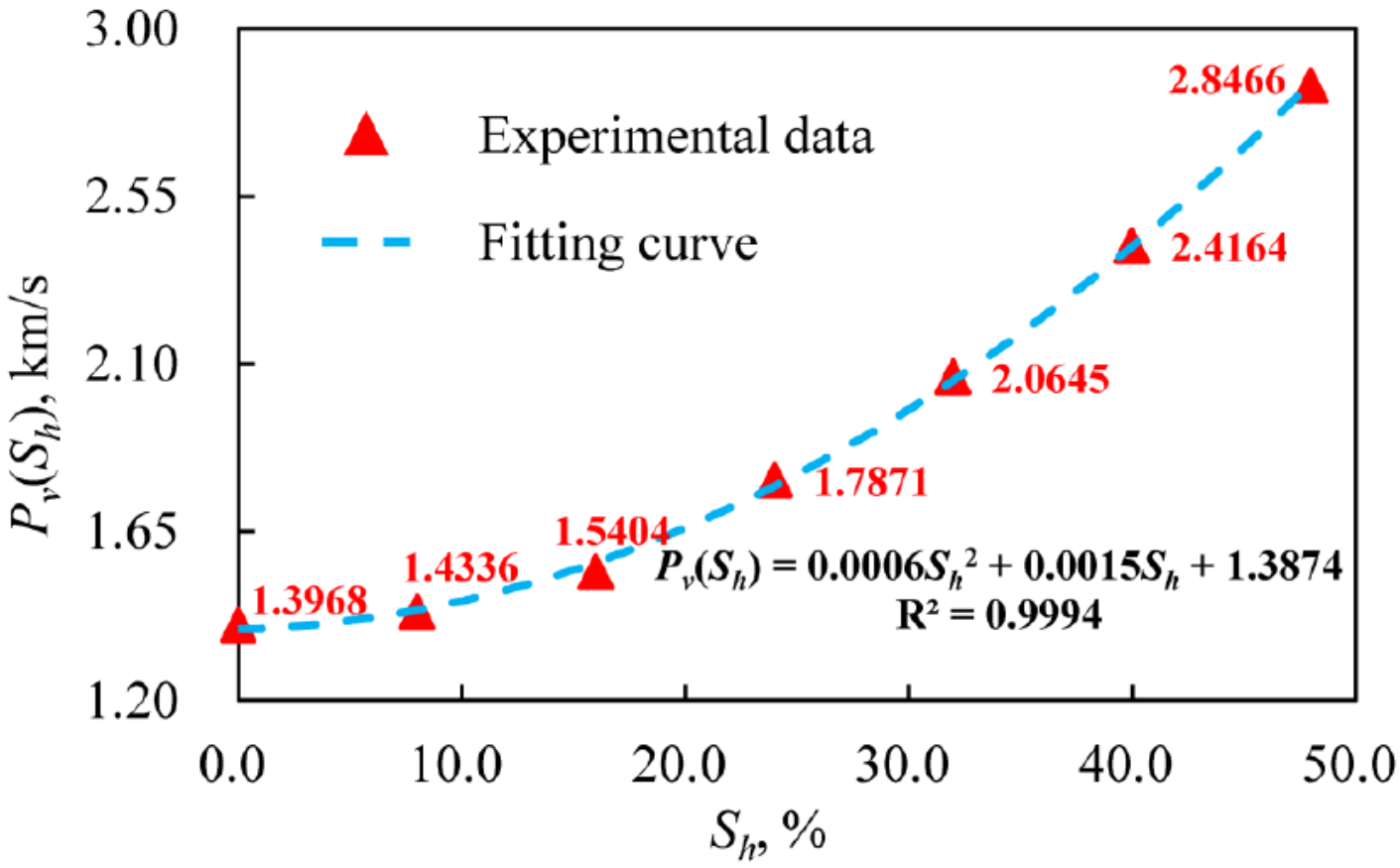

Figure 6

Relationship between acoustic velocity Pv(Sh) and hydrate saturation Sh

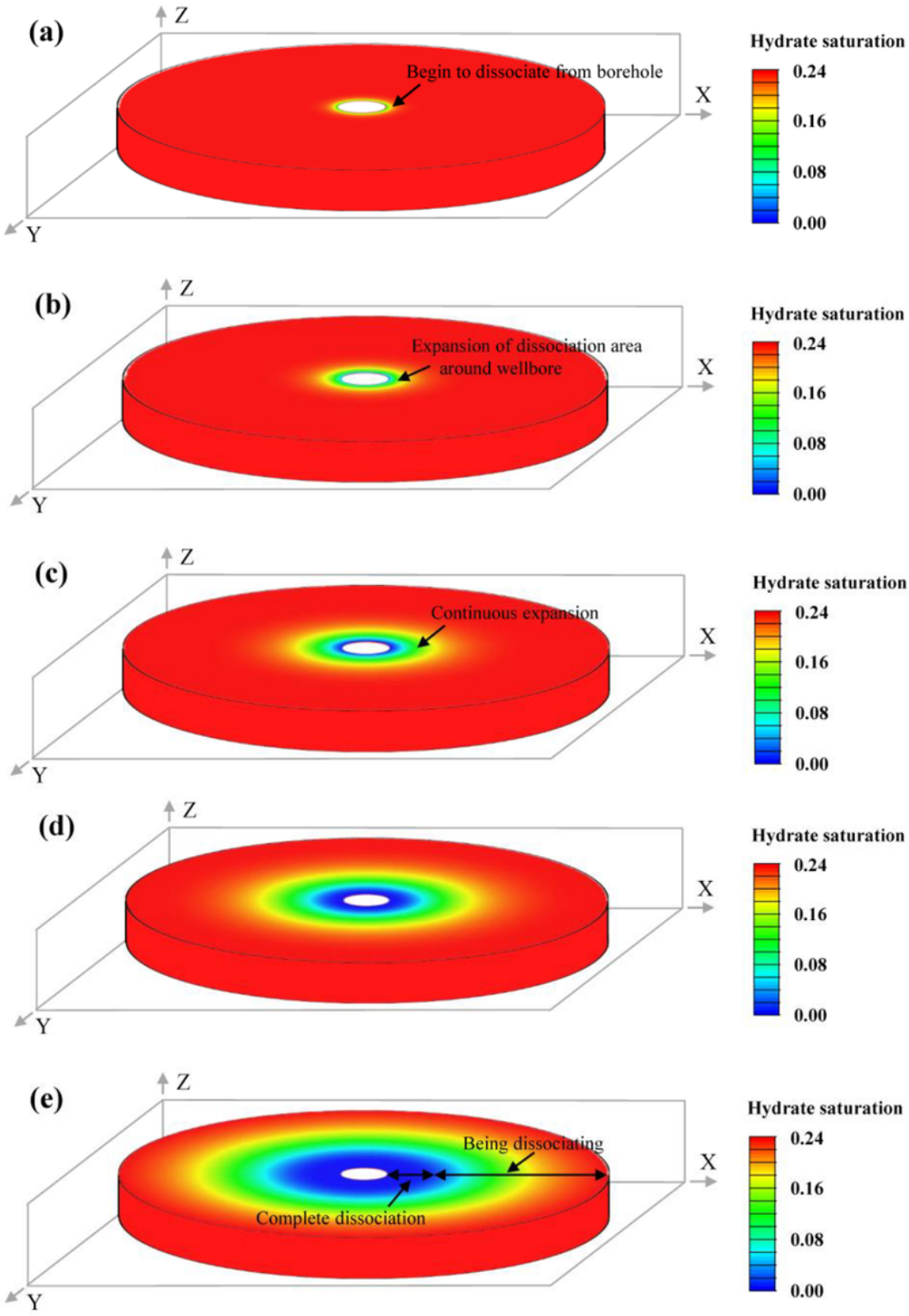

Figure 7

Distribution nephogram of hydrate saturation in sediment at different experimental moments. (a) 0.5h; (b) 2.0h; (c) 12.0h; (d) 24h; (e) 48h

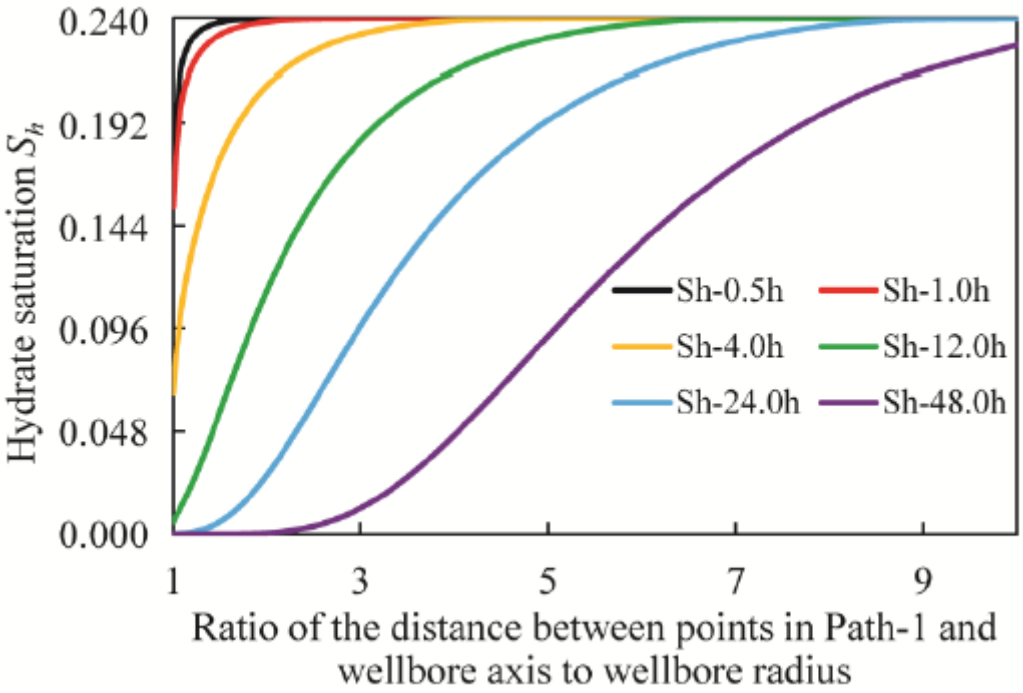

Figure 8

Distribution of hydrate saturation along Path-1 at different experimental moments

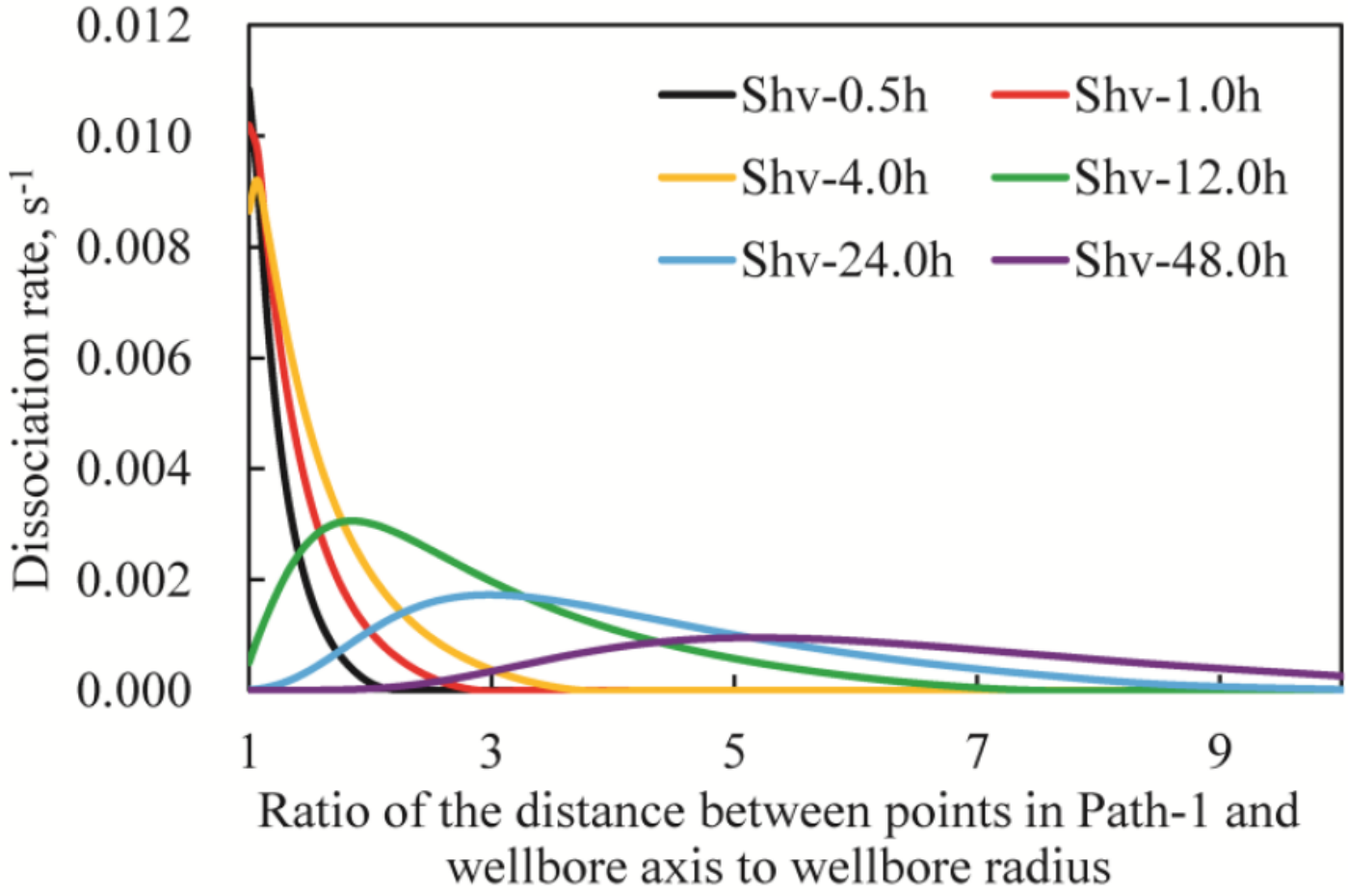

Figure 9

Dissociation rate of natural gas hydrate along Path-1 at different experimental moments

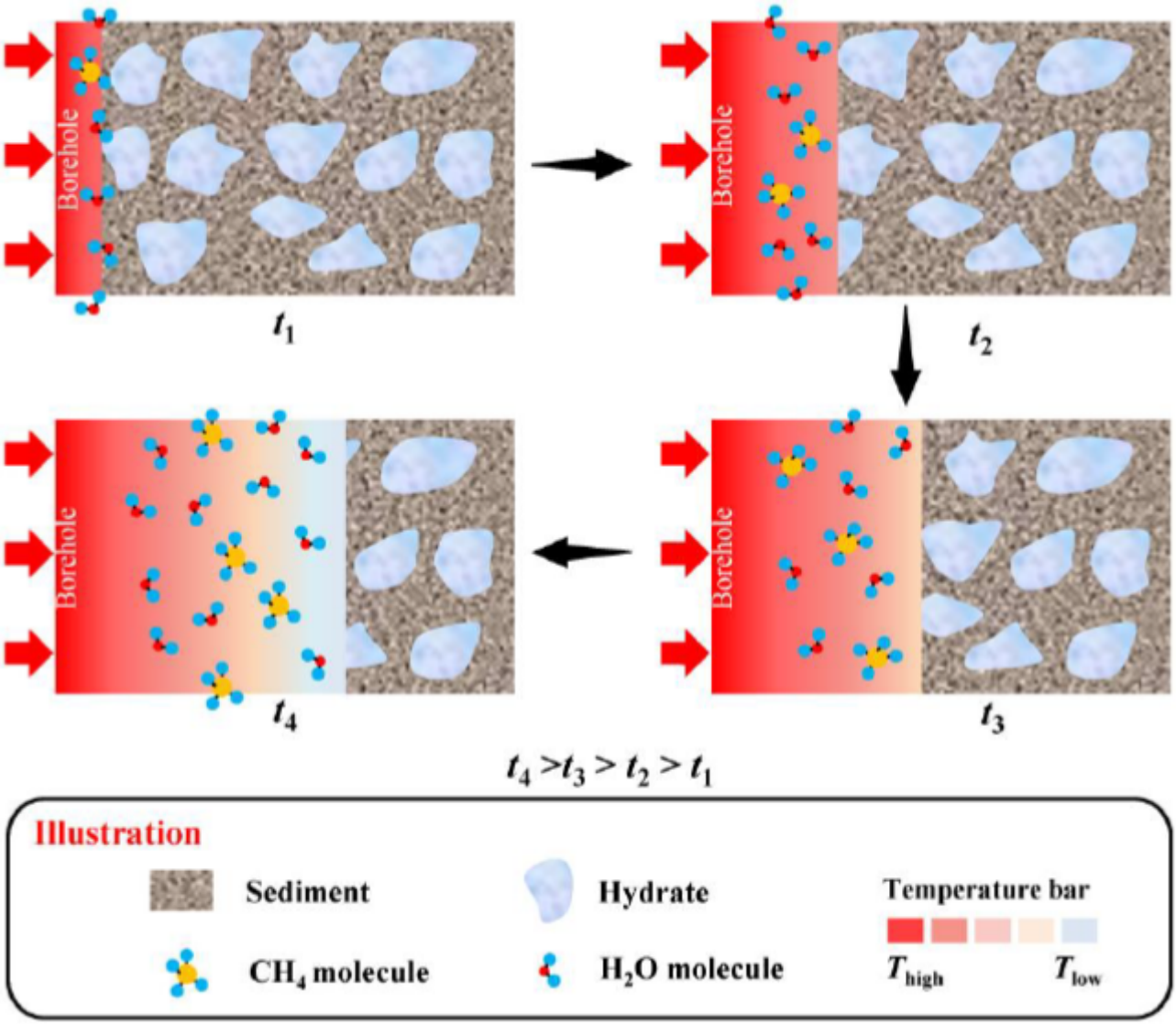

Figure 10

Schematic of temperature distribution around wellbore during hydrate dissociation in near-wellbore region

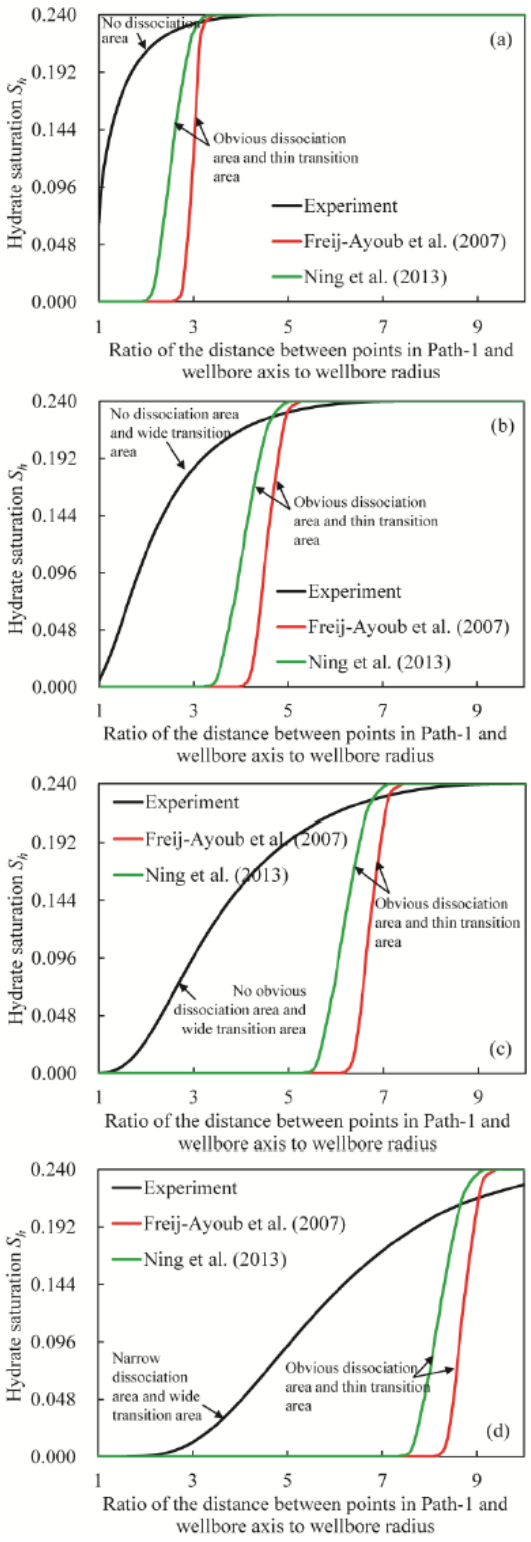

Figure 11

Distribution of hydrate saturation along a radial path around wellbore that obtained by experiment and two simulation methods in different references respectively. (a) 4.0h; (b) 12.0h; (c) 24.0h; (d) 48.0h

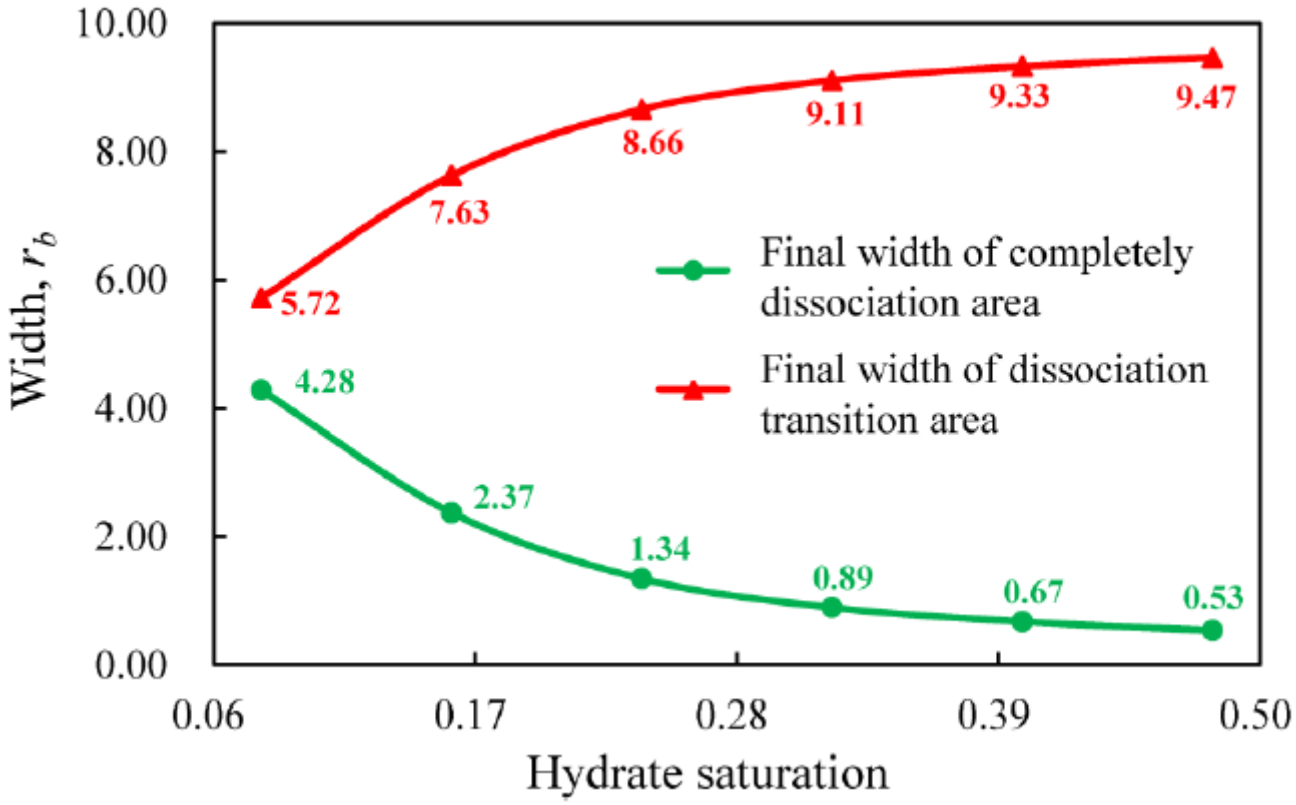

Figure 12

Effect of hydrate saturation on hydrate dissociation around wellbore during drilling operation

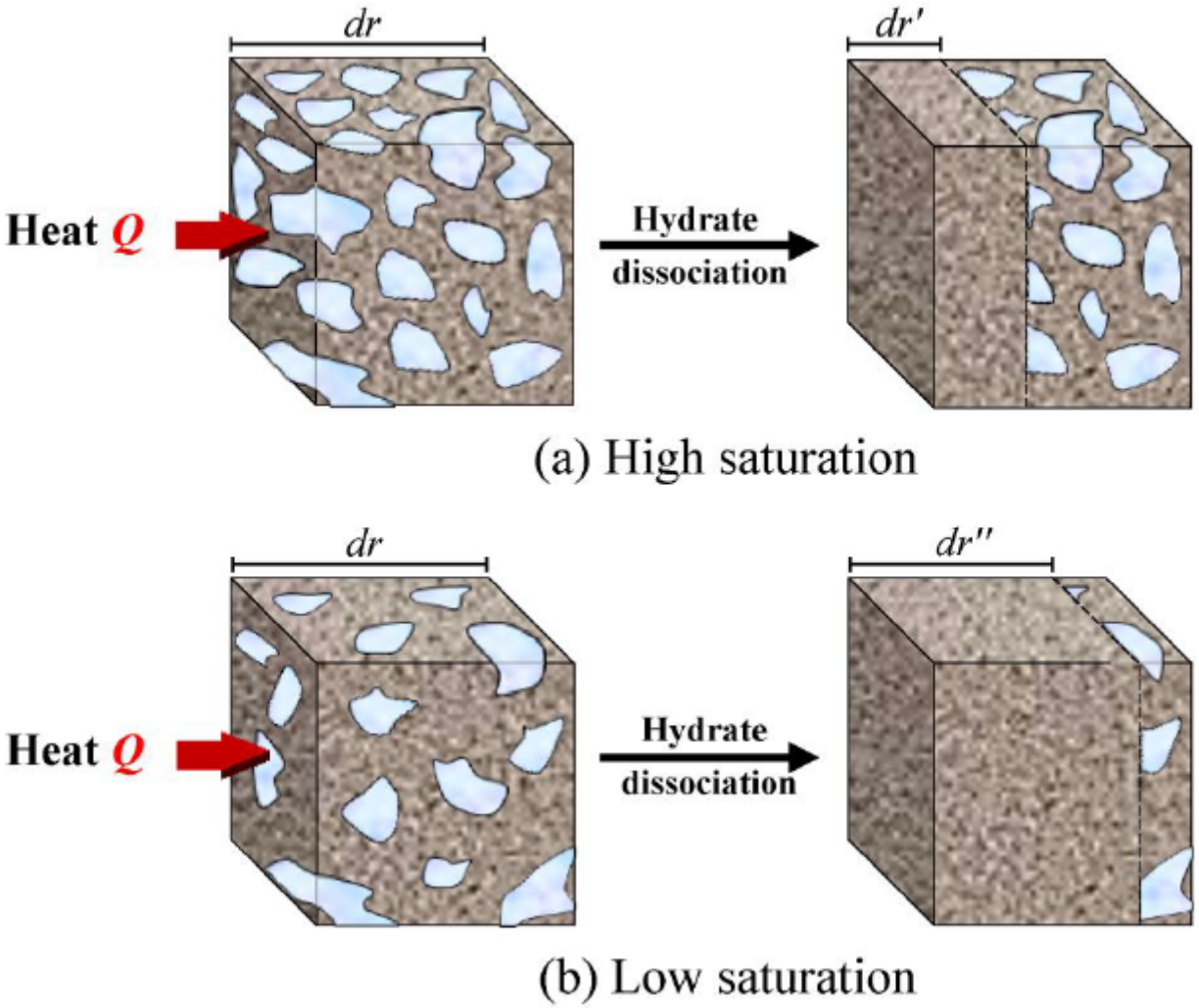

Figure 13

Schematic diagram of the influence mechanism of hydrate saturation on hydrate dissociation in sediments around wellbore

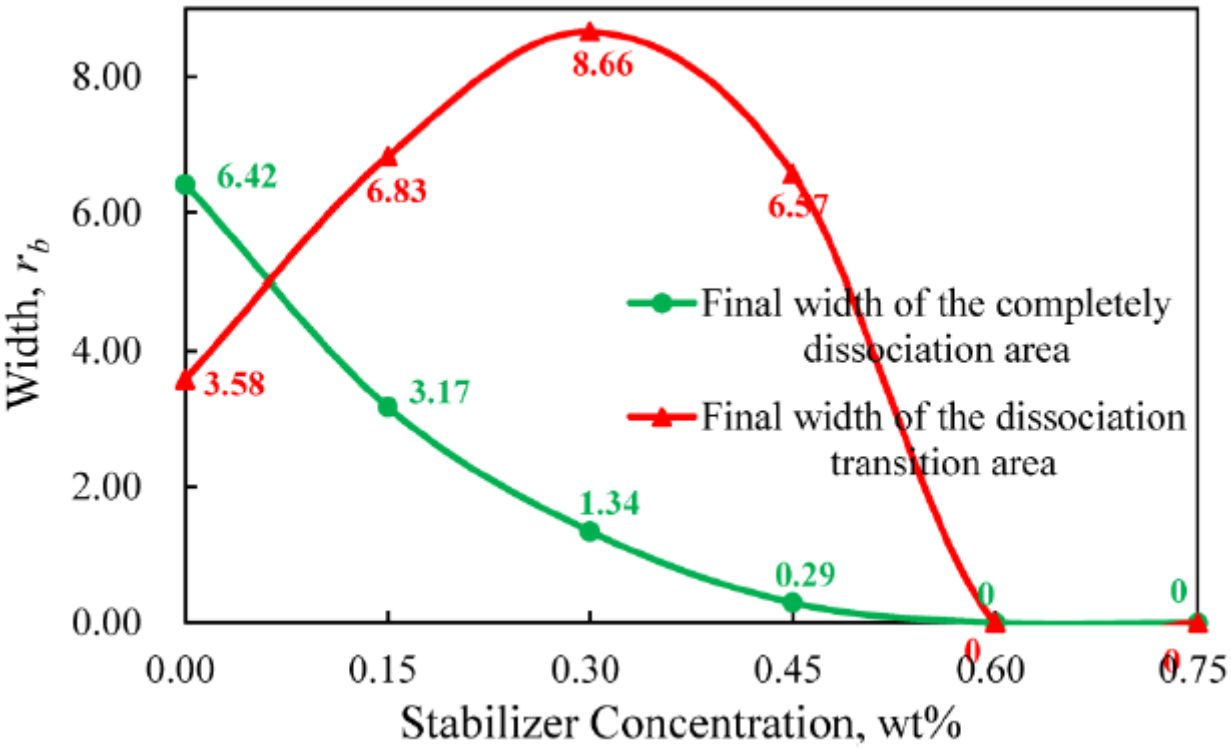

Figure 14

Effect of stabilizer concentration on hydrate dissociation around wellbore during drilling operation

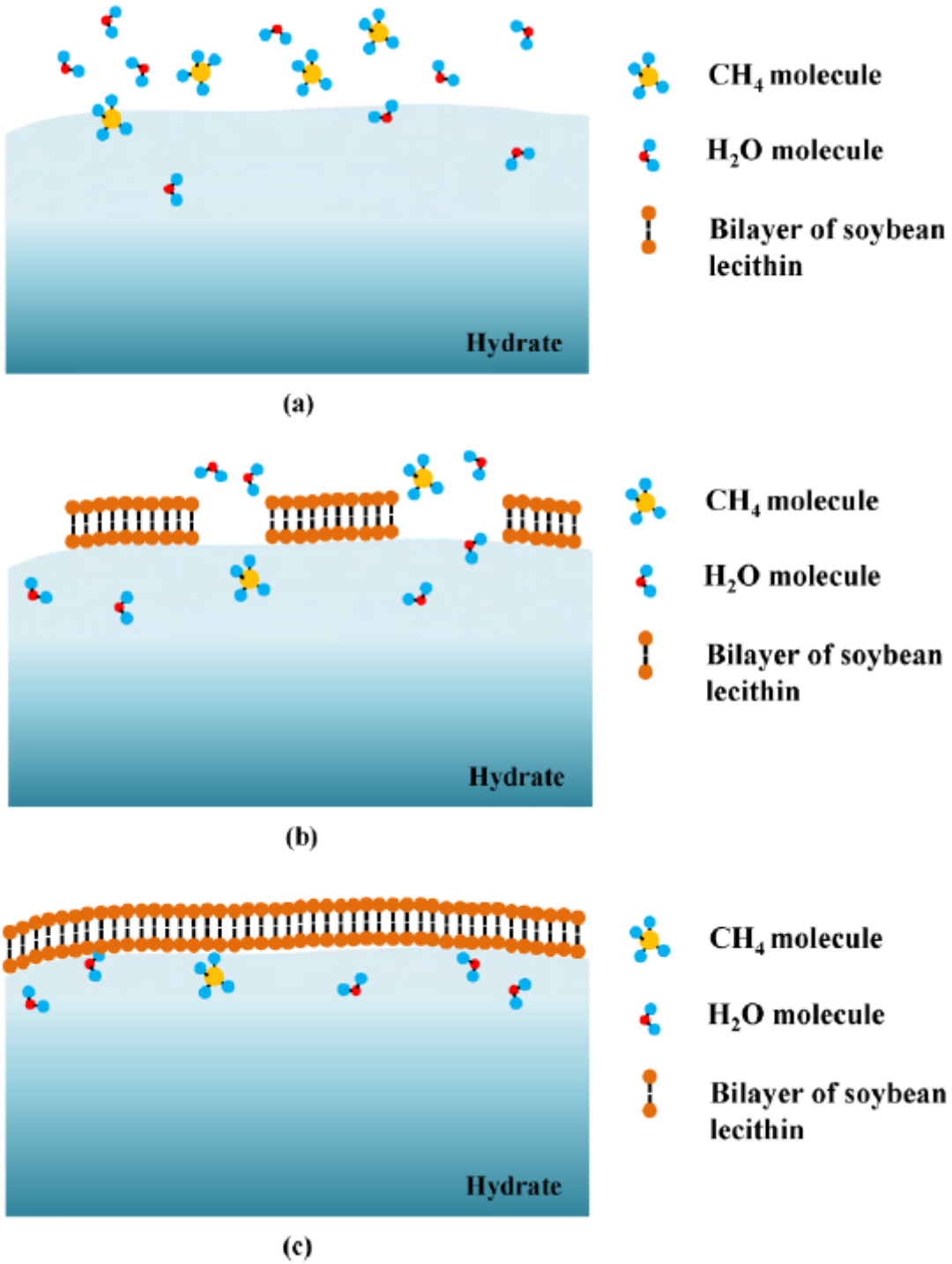

Figure 15

Stabilization mechanism of soybean lecithin on gas hydrate. (a) no soybean lecithin in drilling fluid; (b) low concentration of soybean lecithin in drilling fluid; (c) high concentration of soybean lecithin in drilling fluid